SUPPORTING INFORMATION

Improved graphene blisters by ultrahigh pressure sealing

Yolanda Manzanares-Negro, Pablo Ares†, Miriam Jaafar, Guillermo López-Polín‡*, Cristina Gómez-Navarro, and Julio Gómez-Herrero*

Departamento de Física de la Materia Condensada and Condensed Matter Physics Center IFIMAC. Universidad Autónoma de Madrid, 28049, Madrid, Spain.

Present Addresses

†Department of Physics & Astronomy and National Graphene Institute, University of Manchester. Manchester M13 9PL, UK.

‡Instituto de Ciencia de Materiales de Madrid (ICMM), CSIC. 28049, Madrid, Spain.

Corresponding authors

* E-mail: pablo.ares@manchester.ac.uk, E-mail: guillermo.lp@csic.es

SI1. Difference of the permeation rate for convex and concave configurations

Leakage rate of pressurized graphene drumheads is usually lower in the convex (Figure S1a) than in the concave (Figure S1b) geometry. We attribute this difference to a higher effective adhesion of the membrane with the substrate when the pressure tends to push the membrane against the substrate. Additionally, the elastic energy of the deformed membrane is accumulated on the edges, causing a much higher interaction on this region when the pressure is higher outside the blister. In contrast, when the pressure is higher inside the blister, it will tend to detach the membrane, even causing delamination/peeling of the flake when the pressure is high enough.[1, 2] The difference on the characteristic times for the two geometries varies significantly between different drumheads, but it is around a factor of 1.5 to 3.

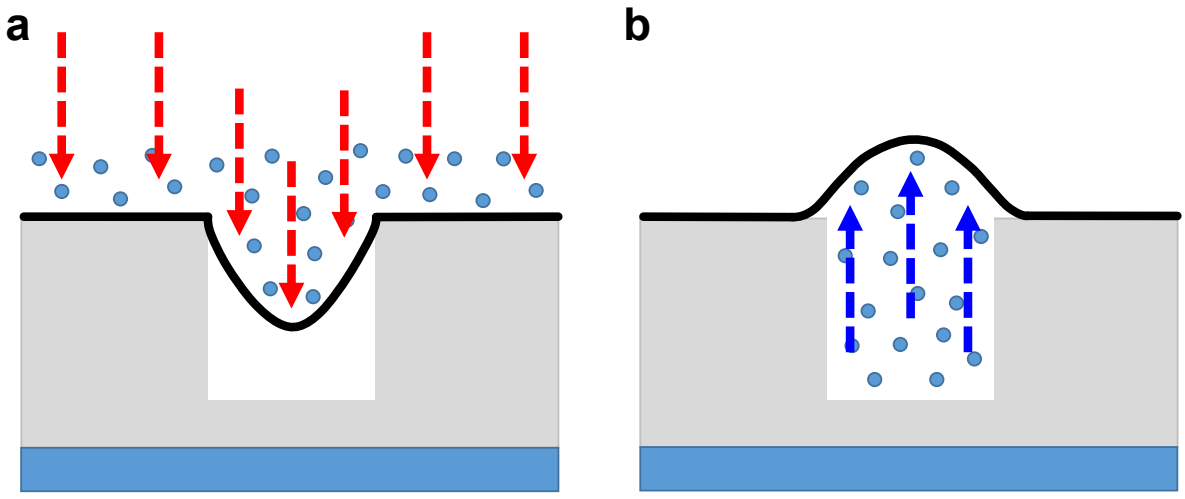

Figure S1. Origin of the difference between the permeation rate for convex (a) and concave (b) blister configurations. For the concave case, if the pressure inside the blister is high enough, it can even produce delamination/peeling of the membrane, facilitating the exit of the gas molecules through the membrane-substrate interface. On the contrary, this will not occur in the convex case, where the higher pressure outside the blister will increase effective adhesion of the membrane.

SI2. Gas diffusion through the graphene-SiO_2 interface

A simple but useful analogy for the behaviour of the gas leakage through the graphene-SiO_2 interface is the gas flow through a cylindrical pipe. As represented in Figure S2, the flow is dependent on the length and the cross section of the tube. Sealing the cavities with a diamond tip is comparable to constrict the tube in some parts, consequently diminishing the leak.

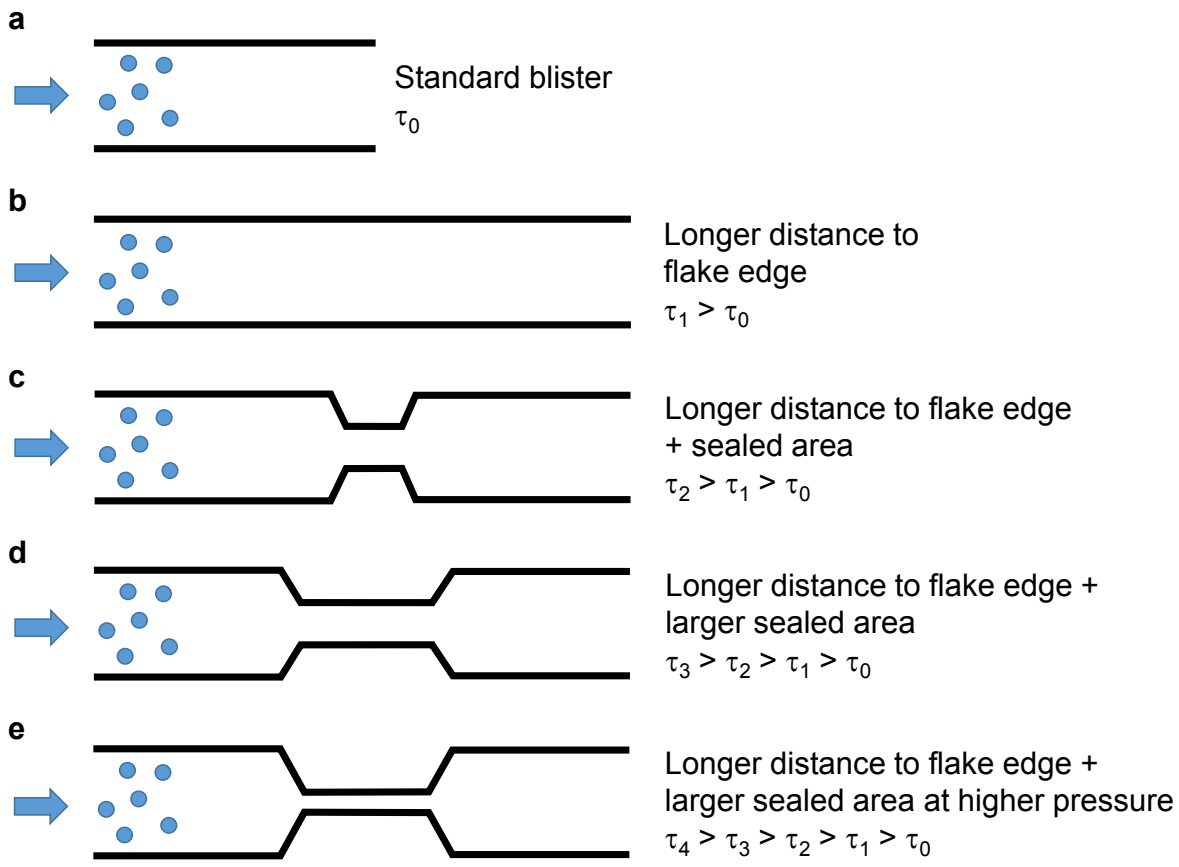

Figure S2. Analogy of the diffusion of gas molecules from the graphene blisters with the diffusion through channels of different length and width. (a) Standard blister. (b) Standard blister with a longer distance to the flake edge. (c) Similar as (b) but with a sealed area around the blister. (d) Similar as (c) but with a larger sealed area. (e) Similar as (d) but with the area sealed using higher pressure.

Poiseuille's law gives the pressure drop in a fluid flowing through a long cylindrical pipe of constant cross section.[3, 4] For a compressible gas, if one of the sides of the tube of radius *r* and length *L* is in high vacuum ($P \sim 0$), the equation describing the volumetric flow rate (*Q*) through the pipe is

$$Q = \frac{dV}{dt} = \frac{1\pi r^4}{28\eta L}\Delta P \quad (1)$$

$$\frac{dV}{dt} = \frac{1dm}{\rho\, dt} = \frac{Mdn}{\rho\, dt} = \frac{MV\, dP}{\rho RT\, dt} \quad (2)$$

Where *V* is the volume, *P* the pressure, ρ the gas density (1.18 kg m^{-3} for air at 298 K), *m* is the mass, *M* is the molar mass of the gas (~ 0.029 kg mol^{-1} for air) and η is the dynamic viscosity of the fluid (1.85×10^{-5} kg m^{-1} s^{-1} for air at 298 K). Combining equations (1) and (2), we get

$$\frac{dP}{dt} = -\frac{\rho RT\pi r^4}{16\eta MLV}P \quad (3)$$

Then

$$P = Ce^{-kt} \quad (4)$$

$$k = {}^{1}\!/_{\tau} = \frac{\rho RT\pi r^4}{16\eta MLV} \quad (5)$$

With τ the characteristic leakage time. For the geometry of a circular membrane, the pressure difference ΔP as a function of the deflection Z can be expressed as[5]

$$\Delta P = \frac{4}{\pi a^2}\left(c_1 S_0 Z + \frac{4c_2 Et}{\pi a^2(1-\upsilon)}Z^3\right) \quad (6)$$

Where *a* is the radius of the pressurized circular region, c_1 = 3.393, $c_2 = (0.8 + 0.062\,\nu)^{-3}$ with ν the Poisson's ratio (~ 0.16), *Et* = 340 N m^{-1} for monolayer graphene and S_0 is the pre-tension accumulated in the sheet. This pre-tension can be very variable from membrane to membrane, with typical values ranging from 0.05 to 0.8 N m^{-1}. [6] Thus, we consider two types of scenarios: membranes dominated by the pre-tension, where

$\Delta P \sim Z$ (valid for small deflections), and membranes dominated by stretching, where $\Delta P \sim Z^3$.

In our measurements, the maximum deflection values are relatively small (typically below 20 nm), so we can initially consider $\Delta P \sim Z$ and hence

$$Z \approx \frac{\pi a^2}{4c_1 S_0} P \tag{7}$$

Then

$$Z \approx \frac{\pi a^2}{4c_1 S_0} C e^{-kt} \;\Rightarrow\; \boldsymbol{Z \approx A e^{-kt}} \tag{8}$$

With

$$A = \frac{\pi a^2}{4c_1 S_0} C \tag{9}$$

$$\tau = {}^{1}\!/_{k} = \frac{16\eta M V L_{eff}}{\pi \rho R T \; r_{eff}^4} \tag{10}$$

As can be seen, the dependence of the height of the blisters follows the same exponential decay we heuristically fitted in the manuscript, with L_{eff} the distance of the blister to the flake edge and r_{eff} the effective radius of a tube that yields the observed leakage rate.

If we now consider the scenario $\Delta P \sim Z^3$, then

$$P \approx \frac{4 \quad 4c_2 E t}{\pi a^2 \pi a^2 (1-\upsilon)} Z^3 = C e^{-kt} \;\Rightarrow\; Z \approx \left(\frac{\pi^2 a^4 (1-\upsilon)}{16 c_2 E t} C\right)^{1/3} e^{-\frac{k}{3}t} \;\Rightarrow\; \boldsymbol{Z \approx A' e^{-k't}}$$

Where $A' = \left(\frac{\pi^2 a^4 (1-\upsilon)}{16 c_2 E t} C\right)^{1/3}$ and $k' = {}^{k}\!/_{3}$

As can be seen, the dependence of the height of the blisters again follows a similar exponential decay.

This toy model yields valuable and still intuitive information of the system. At first glance, this analysis accounts for the linear increase of the blisters gas leakage times with the distance to the flake edge, as observed experimentally (Figure 2d in the main

text). The analysis also allows us to obtain values for the effective radius of the leakage, and thus to better compare leakage rates from blisters in different flakes and leakages before and after sealing. From this analogy, we obtain effective radii for the gas leakage ranging from 0.3 to 1.7 nm before sealing the blisters. Please note that in the scenario where $\Delta P \sim Z^3$, the characteristic time would be $\tau' = {}^{1}\!/_{k'} = 3\tau$. As $r_{eff} \sim \tau^{1/4}$, the differences in the effective radius values obtained from the two scenarios will not be very significant.

SI3. The role of graphene-substrate interaction on the characteristic times of blisters

Together with the distance of the blister to the flake edge or the size of the blister, other effects such as the uncontrolled initial interaction after transfer between graphene and substrate have a strong influence on the inflation/deflation time of the blisters. We performed the experiments described in the manuscript on tens of membranes, getting extremely different results. Figure S3a shows the characteristic times obtained for blisters of similar characteristics (radii *a* between 500 and 750 nm and distances to the flake edge between 2.0 and 2.5 μm) in five different significant samples. It is remarkable that the blisters from samples 4 and 5, where the distances to the flake edge were much higher, 4 and 7 μm respectively, and thus higher times would be expected, exhibit the lowest characteristic times of the plot. Consequently, we attribute this disparity to uncontrolled variations of the graphene-SiO_2 adhesion between different flakes. This is as well reflected on the different effective leakage radii obtained for each of the different samples (Figure S3b).

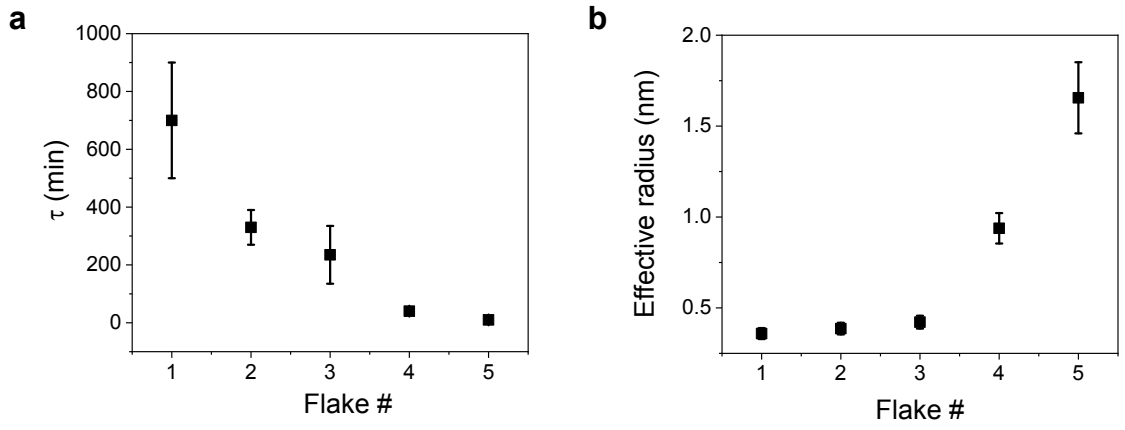

Figure S3. (a) Characteristic times and (b) effective leakage radii of blisters of 5 different samples. The disparity is not related to the distance to the edge, as described above.

SI4. Dimensions of sealed areas

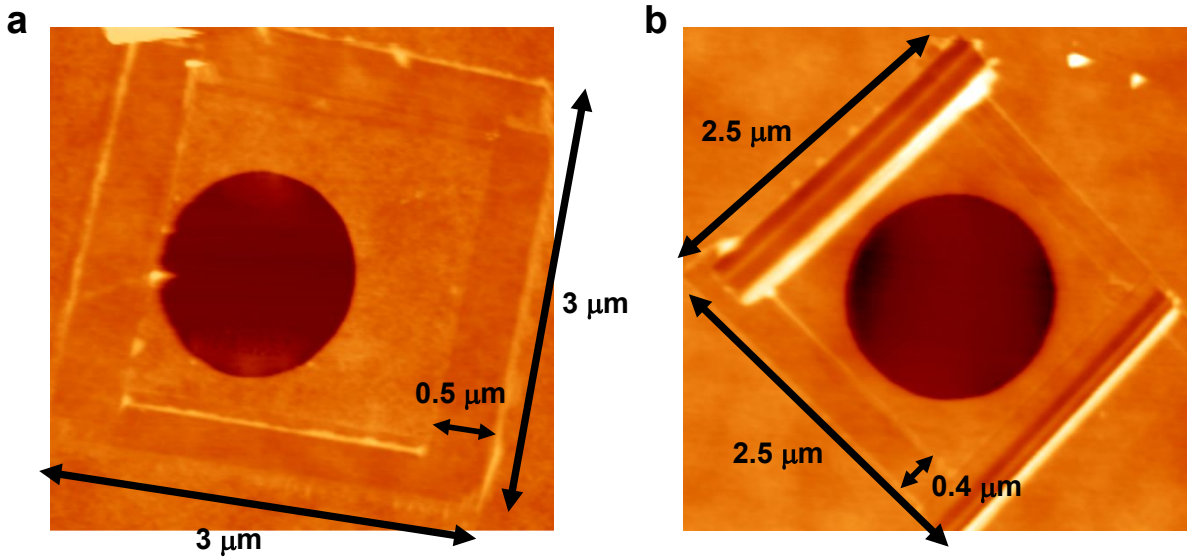

Figure S4. Topographic images of two different sealed blisters with the characteristic dimensions of the sealed areas.

SI5. Increase of graphene-substrate interaction after sealing

The reduction of leakage through the graphene-substrate interface after sealing indicates an increase of the graphene-substrate interaction. This increase upon sealing of drumheads can be very useful for a variety of situations. The total force that a membrane can withstand before breaking under indentation with a tip depends strongly on the radius of the tip. Consequently, the maximum strain produced on the membrane during an indentation is also strongly influenced by the tip radius. Additionally, graphene-substrate interaction can be an issue to achieve high strains, as the membranes tend to sag when applying very high forces.

To gain a qualitative insight on the increase of the interaction between the graphene membrane and the underlying SiO_2 substrate upon sealing, we performed indentations

on sealed and unsealed graphene drumheads using tips with a radius of 250 nm. These especial tips allow us to achieve high average strains necessary to overcome the flake-substrate interaction without breaking the membrane Figure S5a and Figure S5b show images of both drumheads before indentation, where no significant defects such as wrinkles are visible. When indenting the unsealed drumhead at low indentation (Figure S5c), both approach and retract curves overlap, indicating an elastic response of the membrane. For high enough indentations, we can observe a clear hysteresis between the approach and the retract curves (Figure S5e), which is not observed in the sealed case for the same (and even much higher) indentation (Figure S5d). This hysteresis is related to the slippage of the membrane edges during the indentation process. This observation evidences that the sealed drumhead exhibits a much higher interaction with the substrate than the unsealed one. By performing deeper indentations (Figure S5f), we also observe a hysteretic behaviour even in the sealed membrane. AFM images acquired after hysteretic indentations show marked wrinkles in the supported graphene (Figure S5g and Figure S5h), which were not there before, and thus they are the fingerprint of the slippage of the membrane. Our data show that the hysteresis onset occurs at forces almost 3 times higher for the sealed case, confirming a much higher membrane-substrate interaction upon ultrahigh pressure sealing.

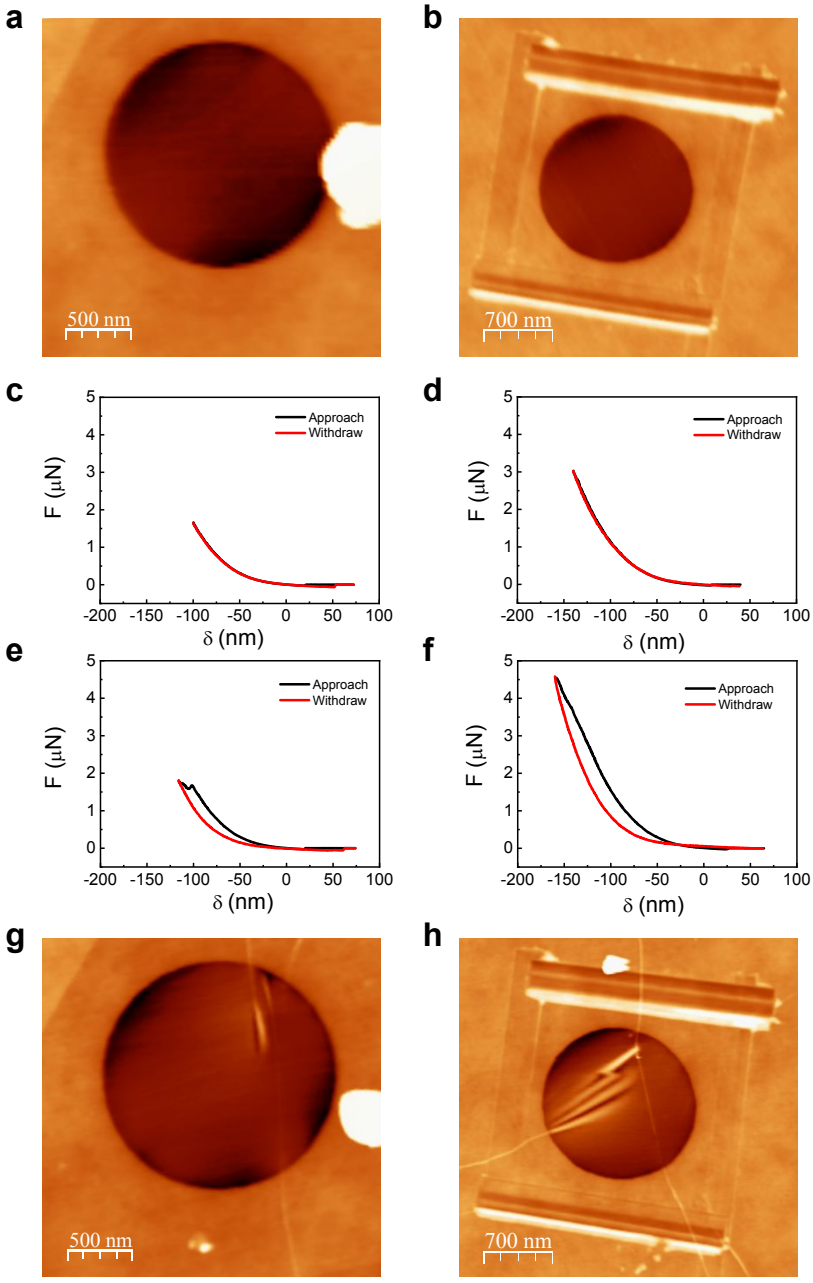

Figure S5. Unsealed (a) and sealed (b) drumheads before high force indentations. Indentation curves for the unsealed (c,e) and sealed (d,f) drumheads. (g) Unsealed and (h) sealed drumheads after high force indentations. Indentation curves are plotted with the same scales for a better direct comparison.

References

1. Boddeti, N. G.; Koenig, S. P.; Long, R.; Xiao, J.; Bunch, J. S.; Dunn, M. L. Mechanics of Adhered, Pressurized Graphene Blisters. *arXiv:1304.1011* **2020**.

2. Koenig, S. P.; G., B. N.; Dunn, L. M.; Bunch, J. S. Ultrastrong Adhesion of Graphene Membranes. *Nat. Nanotechnol.* **2011**, *6*, 543-546.

3. Landau, L.; Lifshitz, E. *Fluid Mechanics*. Pergamon Press: 1987; Vol. 6.
4. Sutera, S. P.; Skalak, R. The History of Poiseuille's Law. *Annu. Rev. Fluid Mech.* **1993**, *25*, 1-20.
5. Bunch, J. S.; Verbridge, S. S.; Alden, J. S.; van der Zande, A. M.; Parpia, J. M.; Craighead, H. G.; McEuen, P. L. Impermeable Atomic Membranes from Graphene Sheets. *Nano Lett.* **2008**, *8*, 2458-2462.
6. Lopez-Polin, G.; Gomez-Navarro, C.; Parente, V.; Guinea, F.; Katsnelson, M. I.; Perez-Murano, F.; Gomez-Herrero, J. Increasing the Elastic Modulus of Graphene by Controlled Defect Creation. *Nat. Phys.* **2015**, *11*, 26-31.